Action Potential of the Motorneuron

Abstract: The excitability of various regions of the spinal motorneuron can be specified by solving the partial differential equation of a nerve fiber whose diameter and membrane properties vary with distance. For our model geometrical factors for the myelinated axon, initial segment and cell body were derived from anatomical measurements, the dendritic tree was represented by its equivalent cylinder, and the current-voltage relations of the membrane were described by a modification of the Hodgkin-Huxley model that fits voltage-clamp data from the motorneuron. In order to compute spike waveforms that match experimental observations, 1) the dendritic membrane must be inexcitable, 2) the voltage threshold of the initial segment of the axon must be ten millivolts lower than that of the cell body, and 3) the density of sodium conductance in the initial segment must be ten times greater than in a typical unmyelinated axon.

Introduction

The spinal motorneuron of the cat holds a preeminent place in our knowledge of neuronal function. Because it is a relatively large neuron its electrical activity can be reliably measured by a micropipette electrode inserted into its cell body. Since it is also the final output device of a mammalian central nervous system, this electrical activity can be correlated with the reflex behavior of the spinal cord. Moreover, several different pathways for activating the motorneuron can be manipulated by the experimenter; for example, excitatory and inhibitory synapses can be activated separately by electrical stimulation of appropriate nerves. Particularly in the work of J. C. Eccles [1,2] and his many collaborators, all these features of the motorneuron have been exploited to give us so detailed a description of its electrical behavior that it is the prototype for interpreting other electrophysiological observations.

More recently, W. Rall [3-6] has extensively developed the mathematical analysis of current flow in branching dendritic trees. An especially important result from that analysis is the demonstration of a class of branching trees equivalent to a uniform cylinder. Anatomical and electrophysiological evidence agree that the motorneuron conforms well to that class. Application of the equivalent cylinder theory has given a qualitative interpretation of the small-signal (subthreshold) equivalent circuit of the motorneuron and has made it possible to use the shape of a postsynaptic potential to estimate how far out on the dendritic tree that synapse is located. In this paper we use this theory to formulate a mathematical model that describes the initiation of the action potential that propagates down the motor nerve.

The main structural features of the motorneuron are diagrammed in Fig. 1 and we will briefly describe their function. The soma, or cell body, which contains the nucleus and most of the cell's machinery for synthesis of macromolecules, is located in the gray matter of the spinal cord. Typically about seven large dendrites leave the soma and branch profusely along their millimeter length. The function of these dendritic trees is to greatly enlarge the surface area on which other neurons can make synaptic connections. When an action potential invades the very small presynaptic terminal, it triggers the release of "packets" of a chemical transmitter. The transmitter acts on the adjacent motorneuron membrane to cause a brief pulse of current to flow into the neuron if the synapse is excitatory, or it causes current to leak out of the neuron if the synapse is inhibitory. The voltage changes resulting from the synaptic currents are distributed over the cell according to the cable properties of the dendritic trees. If there is sufficient depolarization (positive deviation of the internal potential from its resting value) to exceed threshold, an action potential is elicited in the motorneuron. This millisecond-long pulse propagates along the axon (nerve fiber) in a manner analogous to a modern submarine cable in which widely separated amplifiers restore signal energy lost from the intervening passive cable. In the case of the vertebrate myelinated axon, the amplifiers are the nodes of Ranvier, at which points the excitable membrane of the axon is exposed to extracellular salt solution. Elsewhere, the axon behaves as a passive cable because the core conductor is insulated by a thick coating of fatty material, the myelin.

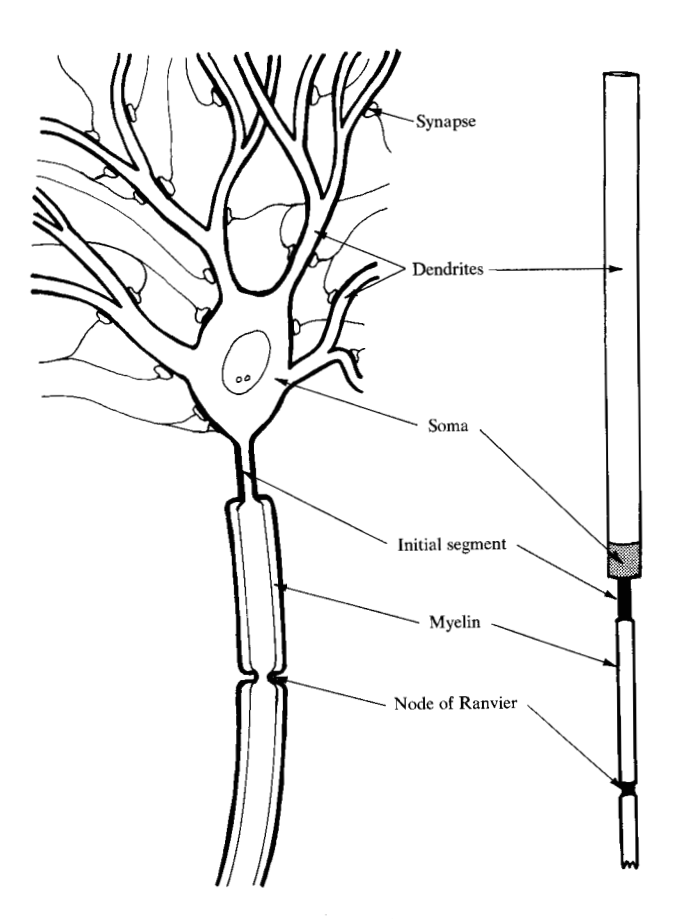


Figure 1 Schematic drawing of a spinal motorneuron, showing a small fraction of all synaptic endings, and a representation of its electrical characteristics by a nonuniform cable.

A key point in Eccles' interpretation of motorneuron excitability is that the spike action potential starts in the unmyelinated initial segment of the axon, and this spike will propagate whether or not the somadendritic membrane fires a spike. The prior firing of the initial segment spike causes a characteristic inflection on the rising phase of the motorneuron spike (Fig. 2). Although this inflection is more prominent when the spike is elicited by electrical stimulation of the motor axon [antidromic activation, Fig. 2(a)], it is also observed during synaptic excitation [Fig. 2(b)] when the soma-dendritic membrane is more depolarized than the initial segment [7]. To account for this, Eccles postulated that the voltage threshold of the initial segment membrane must be about 10 mV lower than that of the soma-dendritic membrane. The relative unimportance of the soma spike is illustrated by the fact that during its period of relative refractoriness, which lasts several milliseconds, the initial segment can generate a propagated spike that is recorded by the microelectrode as a spike less than 50 mV in amplitude. The experiment that most clearly identified the sites of spike generation [Fig. 2(c)] involved stepwise blocking of the components of the antidromic spike by hyperpolarizing the neuron with current applied through the microelectrode [8]. A hyperpolarization of 15 mV blocked invasion of the soma when the 50-mV spike from the initial segment failed to reach the soma threshold; a further 5- to 10-mV hyperpolarization blocked excitation of the initial segment, leaving only the 5-mV deflection generated by the spike of the first node of Ranvier.

The possibility of quantitatively testing this interpretation existed in principle since the results of voltage-clamp experiments by Araki and Terzuolo [9] in 1962, which give specifications for the excitability of the somadendritic membrane. In this paper we use their voltage-clamp data with Rall's equivalent cylinder approximation for the cable properties of the dendrites to make a quantitative model of the motorneuron.

Formulation of the model

• Cable theory for an axon

For most purposes the distribution of membrane potential along a thin cylindrical axon can be described accurately by the one-dimensional cable equation

$$\frac{a}{2R_{i}}\frac{\partial^{2}V}{\partial x^{2}} = I_{m} = C\frac{\partial V}{\partial t} + I_{i},$$
(1)

in which the local value of the radial membrane current density $I_{\rm m}$ is given by the divergence of the longitudinal current (left-hand term), where V is the potential difference across the membrane measured as the departure from its resting value, x is the distance along the fiber, a is fiber radius and $R_{\rm i}$ is the specific resistance of the axon's cytoplasm. But $I_{\rm m}$ must also depend on the local membrane properties; in particular it is the sum of the displacement current through the membrane capacitance $C_{\rm m}$ and the current carried by the movement of ions through the membrane $I_{\rm i}$.

If the membrane is inexcitable, as in myelinated regions, or if the potential changes are so small that the ionic permeability remains constant, then $I_i = V/R_{\rm m}$ where $R_{\rm m}$ is the resistance of a unit area of membrane. In this case, Eq. (1) describes a passive cable, and if the membrane properties and the radius are uniform along the fiber, it can be solved analytically for many boundary conditions of interest. Convenient parameters for describing the behavior of a passive cable are its characteristic length λ , where

$$\lambda^2 = a R_{\rm m}/2R_{\rm i} \tag{2}$$

and the membrane time constant τ_m , where

$$\tau_{\rm m} = R_{\rm m} C_{\rm m}. \tag{3}$$

For our purposes it is also convenient to have the equation for the characteristic impedance looking into the end of a long fiber, namely

$$Z = \{R_{\rm m}R_{\rm i}/[2\pi^2 a^3(1+i\omega\tau_{\rm m})]\}^{\frac{1}{2}}.$$
 (4)

If the membrane is excitable, and the functional dependence of the ionic current upon membrane potential and time has been determined empirically, as was done by Hodgkin and Huxley [10] for the squid giant axon, then Eq. (1) can be solved numerically for excitation and propagation of the nerve impulse [11].

 Equivalent cylinder representation of soma and dendrites

Our problem of modeling the motorneuron is greatly simplified by the fact that its branching dendritic tree conforms well to that class of theoretical trees that are equivalent to a uniform cylinder [3]. For this class we assume that $R_{\rm m}$, $R_{\rm i}$ and $C_{\rm m}$ are constant, and that at each branch point the radii of the two daughter branches $a_{\rm i}$ and $a_{\rm i}$ are such that the parent branch (of radius $a_{\rm i}$) is loaded by its characteristic impedance; that is, $a_{\rm i}^{3/2} + a_{\rm i}^{3/2} = a_{\rm i}^{3/2}$, which follows immediately from Eq. (4).

To apply the equivalent cylinder theory to electrophysiological measurements, Rall showed [5] that passive decay of the membrane potential from an initially nonuniform distribution can be expressed as the sum of exponential decays. In this infinite sum the slowest time constant is τ_m , and the values of the other faster time constants depend only on the length of cylinder relative to its characteristic length λ . For motorneurons, it was found that only the first two terms were required to accurately describe the observed transients yielding representative values of $\tau_{\rm m} = 6$ ms and the length of the equivalent cylinder of about 1.5λ [12]. These same values were found applicable to both large and small motorneurons [13]. Barrett and Crill [14] and Lux, Schubert, and Kreutzberg [15] have used modern cell-staining techniques to re-examine the anatomy of dendritic branching; although they found that dendrites actually taper between branch points, this detail would not be expected to cause a serious departure from the equivalent cylinder model. In order to fix the dimensions of our equivalent cylinder we have taken the empirical values of fiber length $L = 1.5\lambda$ and membrane time constant $\tau_{\rm m} = 6$ ms; we assumed $C_{\rm m} = 1 \mu \text{F/cm}^2$, which is typical of a single thickness of cell membrane and fixes $R_{\rm m} = 6000 \ \Omega \text{cm}^2$; and we assumed the reasonable value of $R_i = 100 \ \Omega \text{cm}$, which value is representative of various vertebrate tissues. We have chosen to simulate a large motorneuron having an input resistance of 1 M Ω . The input resistance of a cylindrical fiber of length L, sealed at both ends, is given by

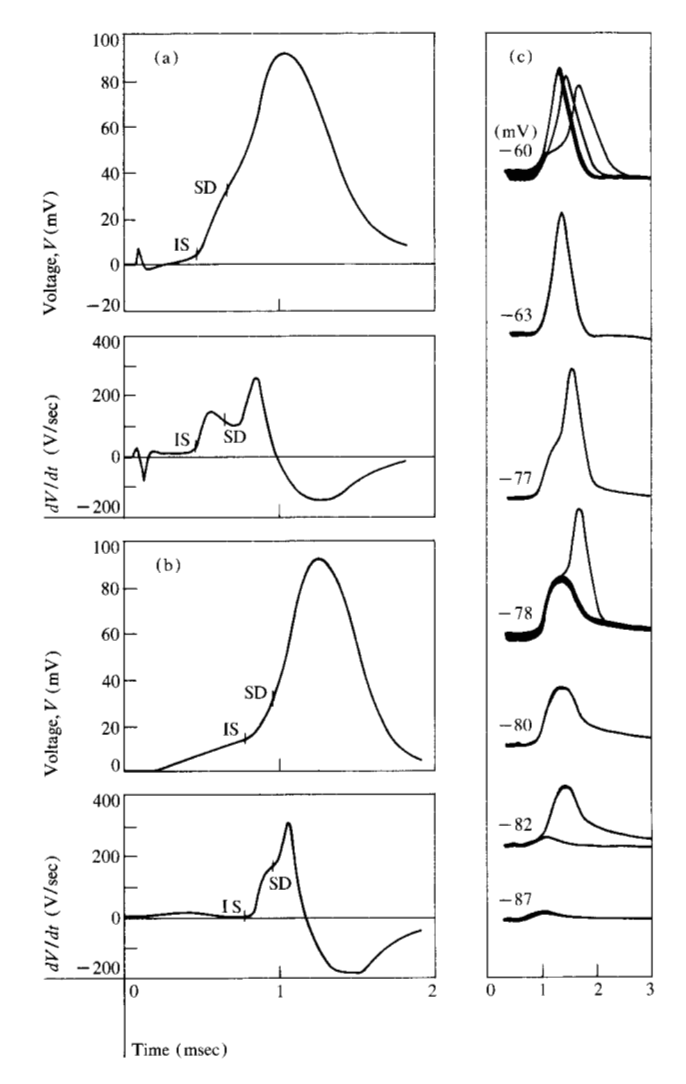


Figure 2 Representative electrical responses recorded by a microelectrode inserted into the soma of a motorneuron. (a) excitation by an antidromic impulse (electrical stimulation of motor axon); and (b) synaptic excitation (Coombs, Curtis, and Eccles [7], 1957; courtesy of the *Journal of Physiology*). Lower traces in (a) and (b) are derivatives of the upper recordings. IS marks the beginning of the initial-segment component of the spike and SD marks the beginning of the soma-dendritic component. (c) Blockage of the antidromic impulse by hyperpolarization of the soma (to the value of resting potential as labeled on trace) by current applied through second barrel of the electrode (Coombs, Eccles, and Fatt, 1955 [8], courtesy of *Journal of Physiology*). Each record consists of several superimposed oscilloscope traces, and at critical voltage levels the record shows both super- and subthreshold responses.

$$R_{\text{input}} = \frac{\lambda R_{\text{i}}}{\pi a^2} \coth (L/\lambda).$$

With the values assumed above, the input resistance is satisfied by a fiber of 30 μ m radius, hence $\lambda = 3$ mm.

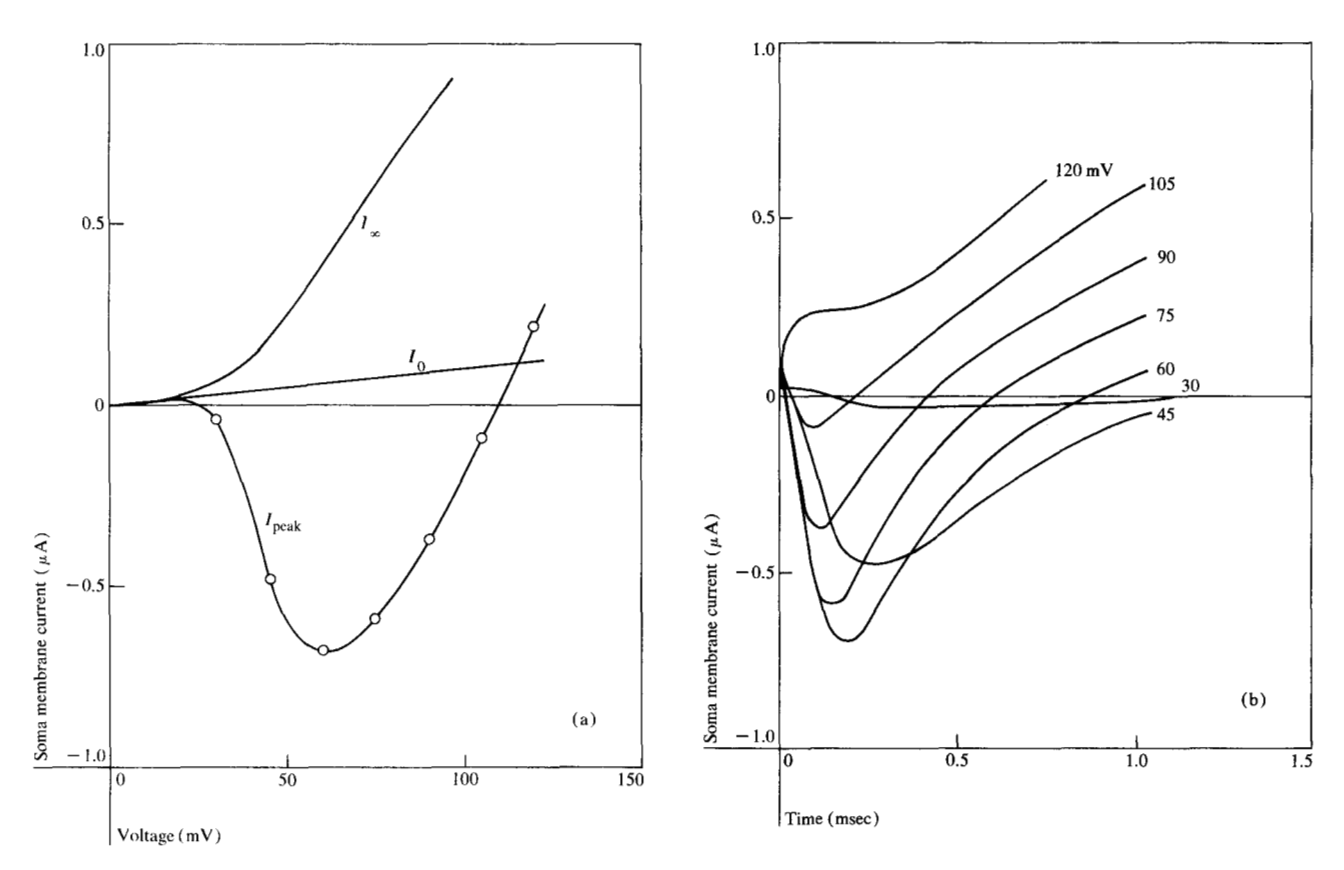


Figure 3 (a) Current-voltage relations of the soma calculated with a modification of the Hodgkin-Huxley equations to fit voltage-clamp measurements on a motorneuron; (b) sample records of current vs time calculated from model.

• Current-voltage relations of excitable membrane

Because the dramatic changes in ionic permeability of excitable membranes are functionally dependent on membrane potential and time, direct quantitative measurement of these parameters can be made only under conditions for which the membrane potential is the controlled variable; i.e., voltage-clamp experiments [16,17]. In the ideal voltage-clamp the membrane potential must be uniform over the area from which the membrane current is measured. In the experiments of Araki and Terzuolo [9], where current had to be injected through another microelectrode, we must expect that the membrane potential of only the soma and basal regions of the dendrites would be under reasonable control. The greater part of the dendrites and the initial segment would not be controlled because of the longitudinal resistance in their cable-like structure [18]. That the presence of the second current-carrying electrode did not damage the cells was indicated by the fact that the motorneuron action potential had normal values for its amplitude and rate of rise.

In the experiment where the membrane potential was clamped to the resting potential and the motor axon was stimulated, antidromic excitation of the initial segment caused a triangular pulse of current about $0.15~\mu A$ in

amplitude and 1 ms in duration to flow into the cell soma. Because the voltage-clamp effectively short circuited the soma membrane, this pulse must represent the maximum stimulus that the initial segment could feed into the electrical load of the soma and dendrites. When the soma potential was commanded to follow stepwise depolarizations, measured current records contained this same triangular pulse if the depolarization exceeded about 15 mV, showing that such depolarizations excited the initial segment spike. The larger transient currents generated by the soma-dendritic membrane were observed during depolarizations greater than about 25 mV. Above this threshold the membrane currents had the sequence of changes typical of the squid axon membrane [17] and of the nodes of Ranvier in vertebrate nerve [32].

To describe the excitability of the motorneuron membrane mathematically we have adjusted parameters of the Hodgkin and Huxley model [10] of the squid axon membrane to fit the current-voltage relations [9] measured by Araki and Terzuolo. In this model, depolarization causes a transient increase in permeability to sodium ions followed by a delayed increase in permeability to potassium ions. The contribution of each ion species to the ionic current depends on the electrochemical potential dif-

Constants in Hodgkin-Huxley equations

$\alpha_m = \frac{0.4 (25 - V)}{\exp[(25 - V)/5] - 1}$	$\beta_m = \frac{0.4 \ (V - 55)}{\exp \left[(V - 55)/5 \right] - 1}$	$V_{\rm Na} = 115 \text{ mV}$
$\alpha_h = 0.28 \exp [(10 - V)/20]$	$\beta_h = \frac{4}{\exp[(40 - V)/10] + 1}$	$V_{\rm K} = -5.0 \ {\rm mV}$
$\alpha_n = \frac{0.20 (20 - V)}{\exp[(20 - V)/10] - 1}$	$\beta_n = 0.25 \exp [(10 - V)/80]$	$V_{\rm L} = 0 \; {\rm mV}$

Nonuniform cable and membrane constants in different regions

	Dendritic equiva- lent cylinder	Soma	Initial segment	Myelin	Node
radius (µm)	30	30	5	8	10
length (µm)	4500	300	100	400	75
$\bar{g}_{\rm Na}$ (mmho/cm ²)	0	70	600	0	600
$\bar{g}_{\rm K} ({\rm mmho/cm}^2)$	0	17.5	100	0	100
$\bar{g}_{\rm L} \ ({\rm mmho/cm}^2)$	0.167	0.167	1	0.05	3
$C_{\rm m} (\mu {\rm F/cm}^2)$	1	1	1	0.05	1
segments	30	6	5	5	1

ference for that ion across the membrane and the permeability of the membrane measured as an ohmic conductance: i.e.,

$$I_{\rm i} = g_{\rm Na}(V - V_{\rm Na}) + g_{\rm K}(V - V_{\rm K}) + g_{\rm L}(V - V_{\rm L}). \tag{6}$$

Excitability of the membrane results from the sodium conductance change since the inward sodium current regenerates the depolarization. The delayed increase in potassium conductance acts to restore the potential to the resting state. The constant "leakage" conductance g_L is taken to be the conductance of the resting membrane of the equivalent cylinder $(1/R_m)$ and V_L is taken as the resting potential $(V_L \equiv 0)$. The dependence of g_{Na} and g_K on time and membrane potential are given an empirical description in terms of the dimensionless variables that describe the activation (m) and the slower inactivation (h) of g_{Na} ,

$$g_{\text{Na}} = \bar{g}_{\text{Na}} m^3 h \tag{7}$$

and the slower activation (n) of g_K

$$g_{K} = \bar{g}_{K} n^{4}, \tag{8}$$

where $\bar{g}_{\rm Na}$ and $\bar{g}_{\rm K}$ are constants, and the subsidiary variables each follow a first-order rate equation of the form

$$dm/dt = \alpha_m (1 - m) - \beta_m m, \tag{9}$$

in which the forward (α) and backward (β) rate constants are monotonic functions of the membrane potential. The rate constants for the motorneuron were modified from the squid model. Like the vertebrate nodes [18] the m process is somewhat faster, while h and n are slower than the squid model at room temperature

(Table 1). Having adjusted the m rate constants to give a threshold at about V=35 mV, we selected a value of $\bar{g}_{\rm Na}$ to give a peak inward current of about $0.7~\mu{\rm A}$ [Fig. 3(a)]. Araki and Terzuolo [9] measured $0.5~\mu{\rm A}$ on a somewhat smaller cell of 1.2 M Ω input resistance. The value of $\bar{g}_{\rm K}$ was chosen to fit the observation that the slope of the steady-state current-voltage relation I_{∞} is about 10 times greater than that of the resting state I_0 . Sample records of current vs time calculated from our model are shown in Fig. 3(b), and these match well the time scale of the motorneuron currents.

If we were to take this model for the soma-dendritic membrane and apply it to the lumped equivalent circuit (a 0.025- μ F capacitor shunted by a 1-M Ω resistor) used by Eccles' group, we calculate a small weak action potential whose rate of rise in less than 100 V/s and which requires a stimulus considerably larger than the maximum current generated by the initial segment. This difficulty should not be taken to imply any deficiency in the voltage-clamp data because, as we see shortly, it is resolved by using the more realistic representation of the electrical characteristics of the soma and dendrites given by an equivalent cylinder.

• Computational methods

Simulation of the motorneuron excitation requires solution of the nonlinear partial differential equation (1) in which the radius of the fiber and several membrane parameters vary with distance along the fiber. To derive a finite difference approximation to this equation we divide the fiber into numerous short, uniform segments of length δx . The membrane current density I_m in the *j*th segment

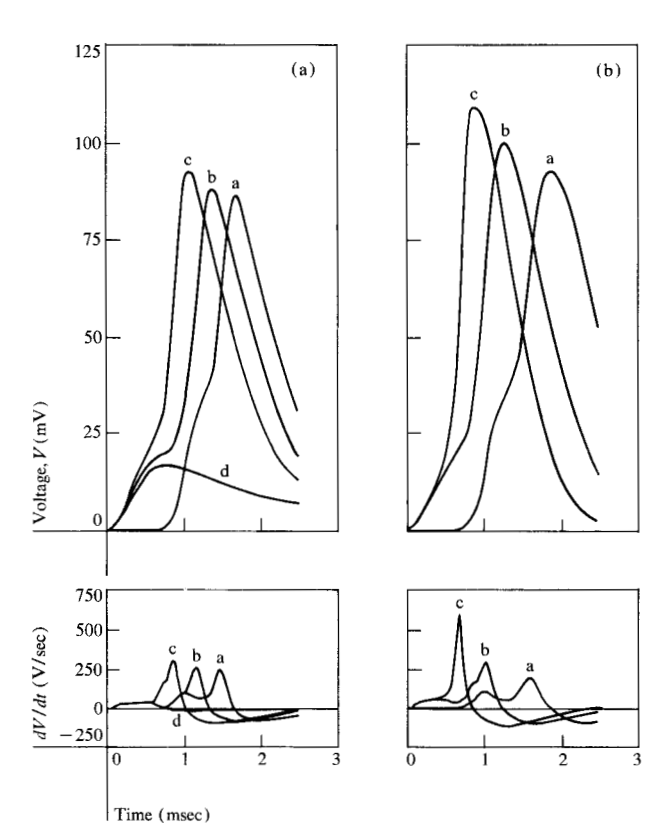


Figure 4 Comparison of a motorneuron model with inexcitable dendrites (a) and with uniformly excitable soma and dendrites (b) for a) antidromic excitation, b) threshold synaptic potential, c) superthreshold (× 1.25) synaptic potential and d) subthreshold synaptic potential. Lower curves are first derivatives of upper.

is given by the difference between the longitudinal current leaving the right-hand edge of the segment and that entering from the left divided by the area of that segment:

$$I_{m_j} = (I_{\log_{j+\frac{1}{2}}} - I_{\log_{j-\frac{1}{2}}})/(2\pi a_j \delta x_j). \tag{10}$$

The consistent finite difference equation for the longitudinal current is the difference between the membrane potentials of adjacent segments divided by the longitudinal resistance between the mid-points of the segments, which is clearly the sum of half the resistance of each segment; i.e.,

$$I_{\log_{j+\frac{1}{2}}} = (V_{j+1} - V_{j}) / \left(\frac{R_{i}}{2\pi} \frac{\delta x_{j+1}}{{a_{j+1}}^{2}} + \frac{R_{i}}{2\pi} \frac{\delta x_{j}}{{a_{j}}^{2}} \right). \tag{11}$$

The boundary condition at the right-hand end of the fiber is zero longitudinal current, which condition corresponds to a sealed end; and at the left-hand end the longitudinal current is a specified function of time corresponding to a stimulus injected through a microelectrode penetrating the otherwise sealed end.

Except for the more complicated difference equations and different boundary conditions, the numerical procedures were essentially the same as those we have previously described [11].

Results

• Excitability of the soma and dendrites

In a voltage-clamp of the motorneuron we do not know precisely which membrane carries the observed current. To the extent that the cell body approximates spherical symmetry, we can expect the potential across the soma membrane to be adequately controlled by current supplied by the servo arrangement. However, in principle, the voltage along the dendrites cannot be controlled since cable theory says that the current which flows into the dendrite must be proportional to the longitudinal voltage gradient. A recent theoretical study by Kootsey and Johnson [18] has shown the limitations inherent in clamping one point of an excitable cable. To model the motorneuron we must therefore consider two cases for the distribution of excitability over the equivalent cylinder. In one case we assume that only the soma is excitable, and in the other case we assume that the somadendritic membrane is uniformly excitable.

Our task of determining the density of ionic conductance was simplified by considering only the equivalent cylinder, which is stimulated at the soma end by a pulse of current equivalent to that generated by antidromic excitation of the initial segment. Even if the membrane is entirely passive, i.e., $\bar{g}_{Na} = 0$ everywhere, a pulse of current 0.15 μ A by 0.5 ms displaces the soma potential about 50 mV, which value is well above the threshold expected from the empirical current-voltage relations.

If only the soma were excitable then the voltage-clamp experiment would measure all the available sodium conductance. Anatomical studies estimate the soma contains from 5 to 10 percent of the total soma-dendritic membrane. If we take all measured ionic conductance and spread it uniformly over the first sixteenth of the equivalent cylinder, then \bar{g}_{Na} is 70 mmho/cm² and we calculate an action potential whose amplitude and rate of rise agree with typical experimental values [curve a of Fig. 4(a)]. We have used these parameter values to represent the case of inexcitable dendrites.

In the case of uniform membrane we found that a density of sodium conductance greater than $\bar{g}_{\rm Na}=35$ mmho/cm² was required to support uniform impulse propagation. Furthermore, a density of at least $\bar{g}_{\rm Na}=50$ mmho/cm² was required to give a soma action potential with an adequate rate of rise [curve a of Fig. 4(b)].

We simulated a voltage-clamp applied to the end of a 20 μ m-diameter excitable dendrite and found that for $\bar{g}_{Na} = 50 \text{ mmho/cm}^2$ the maximum current flowing into

the soma was about $0.08~\mu A$. If we make a realistic neuron model with a $100~\mu m$ -diameter spherical soma and five such large dendrites, then the maximum inward current would not exceed what was observed by Araki and Terzuolo. Therefore, excitability of the dendrites cannot be excluded on the basis of the voltage-clamp data; but we will return to this question after building more of the model.

Initial segment has a high density of sodium conductance

To represent the motor axon in our model we added four more regions along the cable corresponding to the unmyelinated initial segment, the first myelin-covered segment, the first node of Ranvier, and some additional length of axon on which a stimulus was applied to simulate antidromic activation of the neuron. We fixed the dimensions of the initial segment to 10 μ m in diameter by 100 µm in length as values that would probably be measured on the largest motorneurons. We have not found any systematic studies of axonal geometry, but Eccles [1] uses dimensions of 8 μ m \times 80 μ m for the initial segment of his "standard" motorneuron which is somewhat smaller than our simulation, and Lux, et al. [15] show a micrograph in which the axon begins as a uniform cylinder of about 10 μ m diameter. We represent the excitability of the initial segment membrane by the same equations as those for the soma except that the empirical functions for all the rate constants are shifted by 10 mV in order to reduce the threshold.

The adjacent myelin-covered region is assumed to have a core $16~\mu m$ in diameter and $400~\mu m$ long. The thick myelin layer is represented by passive membrane with a capacitance of $0.05~\mu F/cm^2$ and leakage resistance of $20~k\Omega$ cm². The first node of Ranvier is represented by a short segment of excitable membrane with a high density of ionic conductance [32]. We did not set up a realistic model of the myelinated axon because only the first node gives any electrical signal that can be measured in the motorneuron soma. Instead, we simply added a short length of unmyelinated axon to separate the antidromic stimulus from the region of interest.

In Fig. 5 we examine the density of ionic conductance required for the antidromic action potential to invade the soma. We find that the minimum density of sodium conductance is greater than 400 mmho/cm² with the value of 600 mmho/cm² (Fig. 5, curve c) giving the best agreement with typical observations [Fig. 2(a)].

• Soma membrane has an intrinsically higher threshold Because the soma and dendritic membranes are densely covered by synaptic contacts much of that membrane might be occupied by post-synaptic receptor molecules; hence it would be less excitable. Eccles argued that the

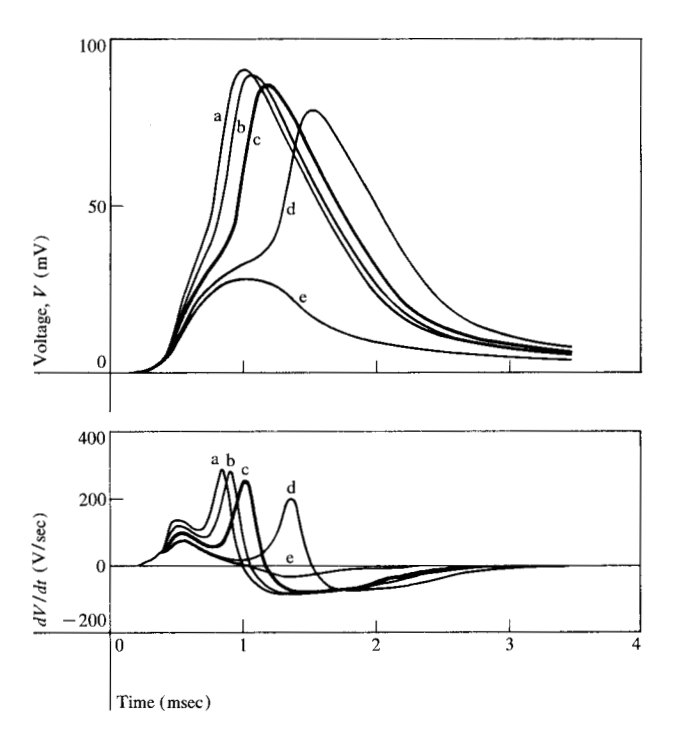


Figure 5 Computed responses of the motorneuron model when the density of sodium conductance in the initial segment was varied from (a) 1000, (b) 800, (c) 600, (d) 500, and (e) 400 mmho/cm²). The density of potassium conductance was 1/6 that of sodium. Lower curves are first derivatives of upper.

presumed lower density of sodium conductance alone could not explain the higher soma threshold because the initial segment fires a spike before the soma, even when the cell is excited by dendritic depolarization [Fig. 2(b)].

Our computations (Fig. 5) have established that the average density of sodium conductance of the soma is in fact very much lower than that of the initial segment. The computations in Fig. 6 establish the validity of Eccles' argument. Here we vary the shift of the membrane potential dependence of the rate constants of the soma while holding all other membrane parameters constant. The stimulus is a step of current applied to the soma. There is no inflection signaling prior to the firing of the initial segment spike if there is no shift. The 10-mV shift (Fig. 5, curve c) used previously best fits typical observations [19].

• Dendrites are inexcitable

Having fixed reasonable values for the parameters of the initial segment we can reexamine the question of dendritic excitability by computing responses to synaptic depolarization of the dendrites. Excitatory synaptic action was simulated by applying a 0.5 msec long pulse of current to the equivalent cylinder at a distance of 0.4 λ from the soma. We chose this distance because it is the

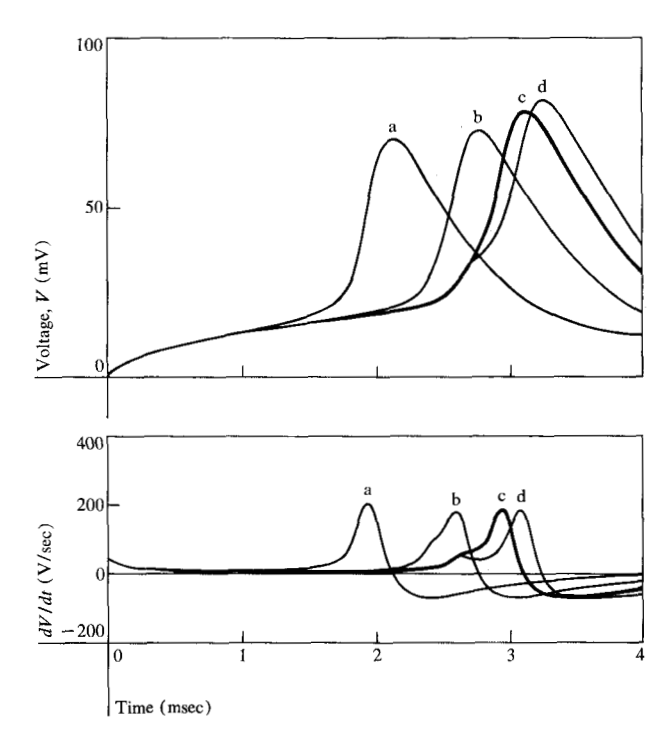


Figure 6 Computed responses of the motorneuron model when the threshold difference between the soma and axon was varied by shifting the rate constants (α and β) in the Hodgkin-Huxley equations of the soma by (a) 10 mV, (b) 5 mV, (c) 0 mV, (d) -5 mV. Curve (c) is the standard value such that the axon has a threshold 10 mV less than the soma. Lower curves are first derivatives of upper.

average value determined for the population of excitatory synapses activated by a stretch reflex [20]. The computed waveform of a subthreshold synaptic potential is shown by curve d of Fig. 4(a). For the case of inexcitable (passive) dendrites in Fig. 4(a) and of excitable dendrites in Fig. 4(b), we compare computed waveforms for antidromic excitation (curves a), a threshold synaptic potential (b), and a larger synaptic potential (c) about 25 percent above threshold. If the dendrites are excitable, normal spike initiation at the initial segment occurs for a threshold synaptic potential. But for a slightly larger synaptic potential, the spike is initiated in the dendrites. When this happens the rate of rise of the soma spike markedly increases to greater than 600 V/sec and the derivative loses the inflection characteristic of the initial segment spike. Normal motorneurons do not behave in this manner, but show only the small changes in spike waveform [Fig. 2(a)] similar to those computed for our model motorneuron with inexcitable dendrites [Fig. 4(a)].

On the other hand, the dendrites of a motorneuron in the abnormal chromatolytic state (see Discussion) are excitable, and such motorneurons commonly show waveforms like those in Fig. 4(b) [21].

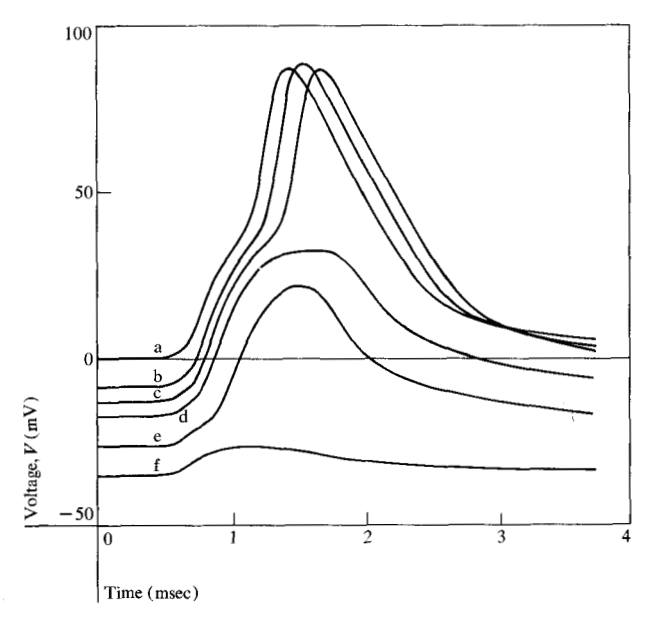


Figure 7 Computation of blockage of antidromic invasion of the motorneuron model by hyperpolarization of the soma by (b)9, (c) 13.5, (d) 18, (e) 17, and (f) 36 mV above the resting potential (a).

• Hyperpolarization block

In Fig. 7 we injected various steady hyperpolarizing currents at the soma end of the equivalent cylinder in order to block invasion of the antidromic action potential. The model and experiment [Fig. 2(c)] agree that a 15 mV hyperpolarization is sufficient to block excitation of the soma. However, the model requires substantially greater hyperpolarization of the initial segment. This small discrepancy could be corrected either by shortening the initial segment or by increasing the resistance between the initial segment and the first node of Ranvier.

• Spatial variations of the membrane current density

Our model can also be used to determine electrical quantities that cannot be measured directly by experiment. For example, a map of the membrane current density is useful for interpretation of the minute voltage gradients measured outside active neurons [22,31]. In Fig. 8 we illustrate the distribution of membrane current during antidromic excitation. In these regions of passive membrane, the dendrites and the myelin, we see only a small predominately outward membrane current, practically all of which is capacitive displacement current. The severe electrical load of the soma and dendrites demands that the initial segment generate relatively large inward current. Our computations show that there is a high density of inward current along all the initial segment, but it is greatest immediately adjacent to the soma where it approaches -5 mA/cm². In its time-course the phase of

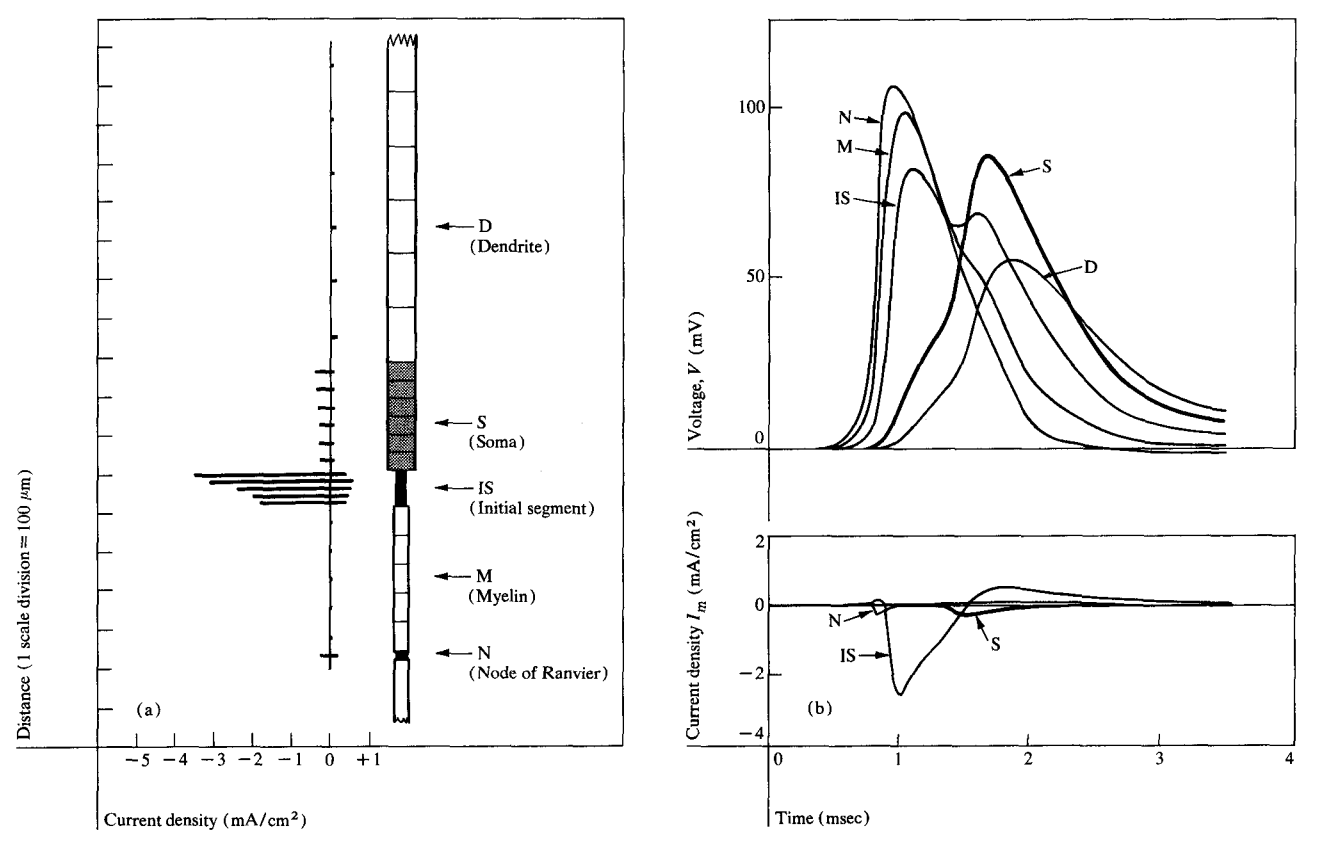


Figure 8 (a) Bar graph of peak inward (-) and outward (+) membrane current density at various points along the motor-neuron model during antidromic excitation. (b) Corresponding sample waveforms of the membrane potential and of the membrane current density.

inward current generated in the initial segment is practically over before the peak of inward current generated by the subsequent excitation of the soma occurs. Its lower magnitude of current density reflects the lower density of sodium conductance in soma membrane.

Discussion

From the electrophysiological observations we infer that an important feature in design of the motorneuron is the convergence of all synaptic influences onto a common point, the initial segment, where the decision to fire a spike is made. Our simulations show that this design is achieved by controlling the spatial distribution of membrane excitability. We find that the spatial gradients in the density of sodium conductance must indeed be very steep, from near zero in the dendrites, to the minimally excitable density in the soma, to a density ten times greater in the adjacent initial segment. This high density is required to ensure excitation of the axon in spite of the electrical load of the soma and dendrites. The initial segment density deduced from our model is about the same as the experimentally determined density in a node

of Ranvier [32]. Furthermore, there is strong, indirect evidence that under the mechanical stress associated with voltage-clamp experiments on a node of Ranvier, the myelin wrapping sometimes lifts away from the axon, revealing the reason that there is no measurable ionic conductance in the axon membrane adjacent to the node [23]. Thus, there is experimental as well as theoretical evidence for a markedly nonuniform distribution of sodium conductance over the neuronal membrane.

The fact that the sodium conductance has a higher voltage threshold in the soma does not imply that these sodium sites differ from those of the axon. Simply because they are more disperse in the soma membrane, they are likely to feel a different local charge density that affects their threshold according to the accepted mechanism for the action of divalent ions on nerve [24].

We can suggest a plausible mechanism to explain how this distribution is developed and maintained. There is accumulating evidence (reviewed by Hille [25]) that each specific ionic conductance arises from discrete macromolecular sites which gate a pore that is more or less selective for a particular ion. In a study of the effects

of denervation on amphibian slow muscle fibers, Miledi, Stefani, and Steinbach [26] found that this normally passive cell became excitable within a few days after nerve section, and that excitability was lost within two months after re-innervation of the cell by the correct nerve fiber. Presumably, denervation of this cell sometimes turns on its biosynthesis of sodium conductance sites in a manner analogous to denervation hypersensitivity in skeletal muscle [27]. If re-innervation of the slow muscle were to stop synthesis promptly, these results suggest that a sodium conductance site has a finite lifetime of about a month or so. We can thus imagine that sodium conductance sites are continually being produced in the motorneuron cell body, where they could be immediately caught up in the axoplasmic flow of macromolecules (reviewed by Weiss [28]), whence they are available to replace any worn out sites in the axon membrane. New sites may be inserted into the initial segment and nodal membrane simply because only these membranes have a strong electric field. Alternatively, R. Llinás suggests (personal communication) that the close apposition of glial membrane to the neuronal membrane might inhibit insertion of sodium conductance sites. This could explain not only the absence of sites under the myelin, but also the intricate patterns of dendritic excitability observed in some neurons of the brain (see e.g., Llinás and Nicholson [29]).

The remarkable changes in dendritic excitability associated with chromatolysis [21] are also explained by the speculations above. The chromatolytic condition results from an enormous increase in the biochemical machinery for synthesis of macromolecules when the cell must regenerate a severed axon. This synthetic activity would presumably cause a higher concentration of sodium sites in the cell body. The density of sodium conductance in the soma membrane increases greatly during chromatolysis as shown by the fact that the antidromic action potential has a much faster rate of rise, although there is no measurable change in the input impedance of the cell [30]. Some sodium conductance sites are also inserted in the dendritic membrane. We cannot offer information about the uniformity of the dendritic excitability, but the existence of small, all-or-none action potentials superimposed on synaptic potentials in chromatolysed neurons indicates that although sodium sites get out to the remote branches of the dendritic tree, the average density remains sufficiently low that blockage of action potential occurs at some point close to the soma.

By using the equivalent cylinder approximation we have been able to estimate values for membrane parameters averaged over gross structural features. We have found a markedly nonuniform distribution and have suggested the implications of this fact with respect to the biology of neural development. We look forward to re-

solving some more questions on the electrophysiology of dendrites by formulating and solving a more realistic model of their tree-like structure.

References

- 1. J. C. Eccles, *The Physiology of Nerve Cells*, The Johns Hopkins Press, Baltimore, Maryland 1957.
- J. C. Eccles, The Physiology of Synapses, Academic Press, New York 1964.
- 3. W. Rall, "Theory of Physiological Properties of Dendrites," Ann. N. Y. Acad. Sci. 96, 1071 (1962).
- 4. W. Rall, "Electrophysiology of a Dendritic Neuron Model," *Biophys. J.* 2 (part 2), 145 (1962).
- 5. W. Rall, "Time Constants and Electrotonic Length of Membrane Cylinders and Neurons," *Biophys. J.* 9, 1483 (1969).
- W. Rall, "Cable Properties of Dendrites and Effects of Synaptic Location," Excitatory Synaptic Mechanisms, Ed. by Andersen and Jansen, Universitetsforlaget, Oslo, 1970, pp. 175-187.
- J. S. Coombs, D. R. Curtis, and J. C. Eccles, "The generation of Impulses in Motorneurons," J. Physiol. 139, 232 (1957)
- 8. J. S. Coombs, J. C. Eccles, and P. Fatt, "The Electrical Properties of the Motorneuron Membrane," *J. Physiol.* 130, 291 (1955).
- T. Araki, and C. A. Terzuolo, "Membrane Currents in Spinal Motorneurons Associated with the Action Potential and Synaptic Activity," J. Neurophysiol. 25, 772 (1962).
- A. L. Hodgkin and A. F. Huxley, "A Quantitative Description of Membrane Current and Its Application to Conduction and Excitation in Nerve," J. Physiol. 117, 500 (1952).
- J. W. Cooley and F. A. Dodge, "Digital Computer Solutions for Excitation and Propagation of the Nerve Impulse," *Biophys. J.* 6, 583 (1966).
- 12. P. Nelson and H. D. Lux, "Some Electrical Measurements of Motorneuron Parameters," *Biophys. J.* 10, 55 (1970).
- 13. R. E. Burke and G. ten Bruggencate, "Electrotonic Characteristics of Alpha Motorneurons of Varying Size," *J. Physiol.* 212, 1 (1971).
- 14. J. N. Barrett and W. E. Crill, "Specific Membrane Resistance of Dye-injected Cat Motorneurons," *Brain Res.* 28, 556 (1971).
- H. D. Lux, P. Schubert, and G. W. Kreutzberg, "Direct Matching of Morphological and Electrophysiological Data in Cat Spinal Motorneurons," in *Excitatory Synaptic Mecha*nisms, Ed. by Andersen and Jansen, Universitetsforlaget, Oslo, 1970, pp. 189-198.
- K. S. Cole, Membranes, Ions, and Impulses, University of California Press, Berkeley and Los Angeles 1968.
- 17. A. L. Hodgkin, A. F. Huxley, and B. Katz, "Measurement of Current-Voltage Relations in the Membrane of Giant Axons of *Loligo*," *J. Physiol.* 116, 424 (1952).
- 18. J. M. Kootsey and E. A. Johnson, "Voltage Clamp of Cardiac Muscle. A Theoretical Analysis of Early Currents in the Single Sucrose Gap," *Biophys. J.* 12, 1496 (1972).
- 19. P. Fatt, "Sequence of Events in Synaptic Activation of a Motorneuron," J. Neurophysiol. 20, 61 (1957).
- J. J. B. Jack, S. Miller, R. Porter, and S. J. Redman, "The Distribution of Ia Synapses on Lumbosacral Spinal Motorneurons in the Cat," in *Excitatory Synaptic Mechanisms*., Ed. by Anderson and Jansen, Universitetsforlaget, Oslo, 1970, pp. 199-205.
- 21. J. C. Eccles, B. Libet, and R. R. Young, "The Behavior of Chromatolysed Motorneurons Studied by Intracellular Recording," J. Physiol. 143, 11 (1958).
- P. Fatt, "Electric Potentials Occurring Around a Neuron During Its Antidromic Activation," J. Neurophysiol. 20, 27 (1957).

- 23. B. Hille, "The Selective Inhibition of Delayed Potassium Currents in Nerve by Tetraethylammonium Ion," J. Gen. Physiol. 50, 1287 (1967).
- B. Frankenhaeuser and A. L. Hodgkin, "The Action of Calcium Ions on the Electrical Properties of Squid Axons, J. Physiol. 137, 218 (1957).
- 25. B. Hille, "Ionic Channels in Nerve Membranes," in *Progress in Biophysics and Molecular Biology*, 21. Ed. by Butler and Noble, Pergamon Press, Oxford 1970, pp. 1-20.
- R. Miledi, E. Stefani, and A. B. Steinbach, "Induction of the Action Potential Mechanism in Slow Muscle Fibers of the Frog," J. Physiol. 217, 737 (1971).
- R. Miledi, "An Influence of Nerve not Mediated by Impulses," in *The Effect of Use and Disuse on Neuromuscular Functions*, Ed. Guttman and Hnik, Czechoslovak Academy of Sciences, Prague, 1962, pp. 35-40.
- 28. P. A. Weiss, "Neuronal Dynamics and Neuroplasmic Flow," in *The Neurosciences, Second Study Program*, Ed. by Schmitt, Rockefeller University Press, New York 1970, pp. 840-850.
- R. Llinás and C. Nicholson, "Electrophysiological Properties of Dendrites and Somata in Alligator Purkinje Cells," J. Neurophysiol. 34, 532 (1971).

- M. Kuno and R. Llinás, "Enhancement of Synaptic Transmission by Dendritic Potentials in Chromatolysed Motorneurons of the Cat," J. Physiol. 210, 807 (1970).
- 31. C. A. Terzuolo and T. Araki, "An Analysis of Intra-versus Extracellular Potential Changes Associated with Activity of Single Spinal Motorneurons," *Ann. N.Y. Acad. Sci.* 94, 547 (1961).
- 32. F. A. Dodge and B. Frankenhaeuser, "Membrane Currents in Isolated Frog Nerve Fiber under Voltage-clamp Conditions," *J. Physiol.* 143, 11 (1958).

Received January 5, 1973

The authors are located at the IBM Thomas J. Watson Research Center, Yorktown Heights, New York 10598.